Published in final edited form as:
Biochemistry. 2011 July 5; 50(26): 5824–5833. doi:10.1021/bi200231x.

Stability of myocilin olfactomedin domain variants provides new insight into glaucoma as a protein misfolding disorder

J. Nicole Burns, **Katherine C. Turnage**, **Chandler A. Walker**, and **Raquel L. Lieberman***
School of Chemistry & Biochemistry, Georgia Institute of Technology, 901 Atlantic Drive NW, Atlanta, GA 30332-0400 USA

Abstract

Myocilin variants, localized to the olfactomedin (OLF) domain, are linked to early-onset, inherited forms of open-angle glaucoma. Disease-causing myocilin variants accumulate within trabecular meshwork cells instead of being secreted to the trabecular extracellular matrix. We hypothesize that, like in other diseases of protein misfolding, aggregation and downstream pathogenesis originates from compromised thermal stability of mutant myocilins. In an expansion of our pilot study of four mutants, we compare 21 additional purified OLF variants by using a fluorescence stability assay, and investigate the secondary structure of the most stable variants by circular dichroism. Variants with lower melting temperatures are correlated with more severe glaucoma phenotypes. The chemical chaperone trimethylamine-N-oxide is capable of restoring stability of most, but not all, variants to wild-type (WT) levels. Interestingly, three reported OLF disease variants, A427T, G246R, and A445V, exhibited properties indistinguishable from WT OLF, but increased in vitro aggregation propensity relative to WT OLF suggests that biophysical factors other than thermal stability, such as kinetics and unfolding pathways, may also be involved in myocilin glaucoma pathogenesis. Similarly, no changes from WT OLF stability and secondary structure were detected for three annotated single nucleotide polymorphism variants. Our work provides the first quantitative demonstration of compromised stability among many identified OLF variants and places myocilin glaucoma in the context of other diseases of protein misfolding.

Glaucoma, a leading cause of blindness from retinal degeneration, is a heterogeneous disorder with complex traits, including an early-onset, inherited form closely linked to mutations in the gene encoding for myocilin (1). Over 70 glaucoma-causing mutations have been documented within the myocilin gene, predominantly within its olfactomedin (OLF) domain, from unrelated families of different racial and ethnic backgrounds (2). Among several of its known locations intra- and extra-cellularly in the eye and throughout the human body (3, 4), myocilin is found in high levels in the trabecular extracellular matrix (TEM), the region of the eye believed to regulate intraocular pressure (5). Missense mutations leading to altered amino acid sequences result in its non-secretion from (6) and intracellular sequestration within (7, 8) trabecular meshwork cells. The molecular mechanism(s) by which mutant myocilin lead(s) to altered fluid flow (9) and increased intraocular pressure, a common risk factor for glaucoma (10), is an active area of investigation (4).

Clues to molecular pathogenesis of myocilin glaucoma come from identification of the sub-cellular localization of non-secreting mutant myocilins. Overexpressed myocilins in cell models form toxic aggregates that colocalize with ER stress markers (11, 12) and eventually,

*Corresponding author (R. L. L.): raquel.lieberman@chemistry.gatech.edu, phone: (404) 385-3663, fax: (404) 894-2295.

Supporting Information Available: Supplemental Figs. S1, S2, and S3 as well as Tables S1 and S2 are available free of charge via the Internet at http://pubs.acs.org.

result in cell death (12, 13). In vitro, aggregates of mutant myocilin are not soluble in Triton X-100 (TX100) (14), and in several model cell systems, some secretion can be rescued when cells are cultured at 30 °C (15–17), an experimental condition known to reduce the rates of cellular protein folding and accumulation of potentially toxic protein. For select mutants tested, the addition of nonspecific chemical chaperones such as glycerol, phenylbutyrate (18), and trimethylamine-N-oxide (TMAO) (19) also improves secretion. Finally, when co-transfected with WT myocilin, aggregates of hetero-oligomers are observed intracellularly, consistent with the general autosomal-dominant inheritance pattern observed for myocilin glaucoma (20).

Based on this data, an attractive model for the pathogenesis of myocilin glaucoma involves a toxic gain-of-function for mutant myocilin in trabecular meshwork cells. In the ER, the proteostasis network assists in nascent polypeptide folding and carefully monitors the folded protein to ensure that only correctly folded proteins continue on the path to maturation and cellular trafficking; otherwise, the degradation process is initiated (21). In the case of mutant myocilin, it may be the case that degradation pathways cannot keep up with the accumulation of newly synthesized mutant myocilins that are largely incompetent for secretion to the TEM, which leads to aggregation and ER stress that cannot be alleviated. Additional support for this pathogenesis proposal comes from the findings that glaucoma does not develop in myocilin knock-out mice (22) nor in individuals with premature stop codons that prevent translation of myocilin entirely (23). Nevertheless, it is noted that the toxic-gain-of function hypothesis for myocilin glaucoma, particularly ER sequestration and stress followed by apoptosis, does not converge all of the available data for wild-type (WT) behavior in cells (24–27) or observations of mutant myocilin effects in transgenic mice (7, 8); thus, additional work in the area is needed.

The purpose of this study is to compare the thermal stabilities of numerous OLF missense mutants with WT OLF to lend further credibility for the categorization of myocilin glaucoma as a protein misfolding disorder. This large disease superfamily includes p53-related cancers (28), SOD1-related amyotrophic lateral sclerosis (ALS) (29), certain subtypes of diabetes (30), lysosomal storage disorders such as Gaucher disease (31–33), among others. A feature common to these disorders is missense mutation(s) in a gene that lead(s) to altered protein behavior, aberrant cellular or extracellular activity, and detrimental downstream effects that ultimately manifest in disease. Complementary to cellular studies, animal model studies, genetic analysis, and clinical diagnosis, biophysical analysis of the behavior of purified mutant proteins in vitro is an integral part of comprehending the underlying genotype-phenotype relationships that contribute to pathogenesis.

The disease-causing mutants selected for this stability study (see Figure 1), which together comprise ~40% of all reported glaucoma-causing myocilin mutations (2), have been evaluated previously for aggregate solubility in TX100 (14, 34) and/or temperature-sensitive secretion (16, 17). We also studied three amino-acid altering single nucleotide polymorphism (SNP) variants, which appear in at least 1% of the population (35). These OLF variants are presumed to be benign, and one had been investigated in the solubility assay. Two major disadvantages of the study of OLF, especially compared to p53 or SOD1, are the inability to postulate a correlation between mutation and function, or to categorize mutations by mapping their location on the three-dimensional structure of the protein. Unfortunately, homology modeling with distantly related structural models only covers half of the available OLF sequence, and in these models, the cysteine residues known to form a disulfide bond (36, 37) are not proximal to each other (not shown). Nevertheless, the new stability data set presented here provides the first quantitative demonstration of compromised stability among most, but not all, reported OLF variants, and combined with

results of previous assays and age of glaucoma diagnosis, expands the possible disease mechanisms for myocilin glaucoma in the context of a protein misfolding disorder.

Experimental Procedures

Expression and Purification of maltose binding protein (MBP) – OLF fusion and corresponding mutants

The plasmid for the MBP-OLF fusion was cloned as we described previously (36). Mutant MBP-OLFs were generated by site directed mutagenesis (QuikChange, Stratagene) using the primers listed in Supporting Table S1. Mutated plasmids, verified by DNA sequencing (MWG Operon), were transformed into Rosetta-Gami 2(DE3)pLysS cells (Novagen), cultured, induced, and harvested, as described (36). Procedures for isolation and purification also followed closely procedures described in ref. (36). Briefly, after lysis by French Press and ultracentrifugation to remove all cell debris and insoluble materials, MBP-OLFs were purified using an amylose affinity column and further fractionated into two major species by size exclusion chromatography (SEC), namely, cytosolic aggregates that elute in the void volume and a monomeric species that elutes at the expected retention volume for the fusion protein, ~72 kDa (Supporting Figure S1). The intensity of the monomer peak was highly variable among the mutants described in this study (Supporting Figure S1), but consistent within preparations of each mutant, as noted previously (36). Two variants, P370L and W286R, could only be isolated as aggregates; insufficient quantity of monomer could be isolated for further study. SEC results were normalized by first subtracting the baseline absorbance and then dividing by the highest absorbance value observed in the chromatograph. Purified MBP-OLFs used in experiments were stored continuously at 4 °C and used within three days.

Cleavage of MBP-OLF to isolate OLF proteins for circular dichroism (CD) experiments (below) was accomplished by overnight (~16 h) incubation at 37 °C (wild-type MBP-OLF and mutants G246R, E352Q, E396D, K398R, A427T, and A445V) or room temperature (mutants V426F, Y437H, and I499F) with Factor Xa (New England Biolabs or Roche) in 50 mM Tris pH 8 or 50 mM Hepes pH 7.5, 100 mM NaCl, 5 mM $CaCl_2$. Cleaved OLF variants were fractionated from uncleaved material and MBP by amylose affinity purification followed by fractionation of the unbound material by using a Superdex 75 GL column (GE Healthcare) at 4 °C, to remove all traces of Factor Xa. Cleaved OLFs were subjected to CD analysis immediately after purification.

Differential scanning fluorimetry (DSF)

The stability of OLF variants in the context of MBP-OLF was assessed using a sensitive, quantitative, and relatively high-throughput SYPRO orange (Invitrogen) fluorescence melt assay that follows the increase in accessible hydrophobic regions as a protein is unfolded (36). The addition of 50 mM maltose, which binds to and stabilizes MBP only, serves to shift the melting temperature (T_m) of MBP completely out of the range for OLF (67 °C), and conveniently enables an independent, and simultaneous, measurement of the T_m for MBP and OLF (36). MBP-OLF variants were subjected to this assay in at least triplicate using a Step One Plus (Applied Biosciences) Real Time (RT)-PCR instrument, as described (36). Data were analyzed using Graphpad Prism software as detailed in (38) to identify the midpoint of the transition, the definition of T_m

The DSF assay was also used to monitor the responses of OLF variants to 3M TMAO (Supplemental Figure S2), an osmolyte found previously to be stabilizing for both wild-type and select mutants (36). TMAO is a small molecule thought to exert its stabilizing influence mainly on the peptide backbone rather than the side chain (39), and thus would be expected

to stabilize all variants to the same extent. The inability of 3M TMAO to rescue proteins to wild-type levels (without TMAO) was used as a guideline to cluster the least stable OLF variants (see below).

Circular dichroism (CD)

To compare secondary structure of selected cleaved OLF variants (5–10 μM) with WT OLF, CD spectra were acquired at room temperature on a Jasco J-810 CD spectropolarimeter. Samples were prepared in 10 mM Na/K phosphate, 0.2 M NaCl, pH 7.2 and placed in a 0.1 cm cell for data collection. Thirty to forty consecutive scans ranging from 200 nm to 300 nm, using a bandwidth of 1 nm at a continuous scanning rate of 500 nm/min, were averaged for each sample. Each spectrum was background-subtracted and converted to mean residue ellipticity, $[\Theta]= M_{res} \times \Theta_{obs}/(10 \times d \times c)$ in which $M_{res} = 112.9$ is the mean residue ellipticity (based on protein sequence), Θ_{obs} is the observed ellipticity in degrees at specific wavelength, d is the pathlength in centimeters, and c is the protein concentration in g/mL. Melts for V426F, Y437H, and I499F variants were conducted in duplicate and were analyzed using Boltzmann sigmoid analysis as described (40).

Statistical analysis

Statistical analyses were performed using Graphpad Prism software. Where appropriate, Pearson's correlation is reported and considered significant at a level greater than α=0.05. Unpaired and one sample t-tests were also conducted and two-tailed p-values considered significant if less than or better than 0.05. For the correlation of age of diagnosis versus T_m, the average T_m value for explicitly reported diagnosis ages were included for analysis. Otherwise, no reported data were excluded from Table 1 prior to analysis.

Results

All of the monomeric OLF mutants tested in this study unfold in the range of T_m = 40–55 °C (Table 1, Figure 2) with a precision within ~1 °C. We estimate the accuracy of the DSC T_m measurement to within 2 °C. This evaluation is based on previous work comparing T_m results for wild-type OLF obtained by DSF with T_m values obtained by traditional biophysical techniques such as CD and tryptophan fluorescence melts (40) as well as in this work, in which the unfolding of three OLF disease-causing variants (V426F, Y437H, and I499F; Supporting Figure S3 and Table S2) were examined by CD. Spectra of V426F, Y437H, and I499F are similar to wild-type OLF (Supporting Figure S3a), namely the beta;-sheet signature ~ 214 nm and the β-turn shoulder at ~230 nm (40), and for melts, minor deviations were observed in T_m of the main 214 nm feature compared to DSF (Supporting Table S2). A limitation of the accuracy of T_m values obtained for aggregation-prone OLF by any method is that conditions for reversibility of the transition have not yet been identified. However, in addition to using different methods to measure the T_m, the scan rate dependence for several techniques has been examined (40), and experiments here were conducted at the same slow rate consistent with unfolding under microscopic equilibrium conditions.

Least stable variants (Group A)

The least stable OLF variants include K423E, I477N, and Y437H, with T_m values of ~40 °C by DSF ((36) and Table 1, Figure 2, Group A). Included in Group A are also the two variants for which no monomeric protein could be isolated. The stability of the three isolated variants could not be rescued to wild-type levels by TMAO (Table 1, Supplemental Figure S2), but are folded proteins with minimal perturbation in secondary structure observed by CD (see () and Supplemental Figure S3). In relation to previous results using TX100 solubility to characterize myocilin aggregates (Table 1), these OLF mutants were found to

generate insoluble aggregates. Likewise, the variants in Group A showed no secretion at 37 °C, and little, if any, secretion at 30 °C. Finally, these variants are associated with the overall earliest ages of glaucoma diagnosis. The mutation associated with the earliest age of diagnosis, 10 years, is P370L. The I477N and K423E mutants have been diagnosed as early as age 18 and 19, respectively. For Y437H, the range of diagnosis is 8 to 41 years (41).

Notably, K423 and Y437 are strictly conserved among myocilins from related mammals such as mice, rat, fish, and cows (Figure 1). Given the fact that the mutation results in an amino acid of similar size to the wild-type amino acid, side chain interactions and properties are likely important at these sites. For example, as indicated by the different melt profiles observed for 214 nm and 229 nm (Supporting Figure S3c, T_m values in Table S2), Y437H melts in a less cooperative manner compared other variants (Supporting Figure S3b,d) and WT OLF (40), suggestive of non-native interactions. Likewise, K423 may be located within the interior of the protein, where positive charge is would be stabilized by a neighboring anionic charge. By contrast, I477 is not conserved (Figure 1). Val and Leu are found in this position in *D. rerio* and the non-ocular OLF domain, *S. purpuratus* amassin, respectively, suggesting I477 is located in a hydrophobic pocket that cannot accommodate a polar residue such as Asn.

Moderately stable variants (Group B)

The majority of OLF variants lie in the mid-range of stability, greater than the most severe mutants and statistically less stable than WT, between T_m = ~ 42–48°C (Table 1, Figure 2, Group B, p-value < 0.0001). Variants in this group include changes in size, polarity and charge and overall, in the absence of knowledge of how the mutations map on the three dimensional structure of OLF, it is not straightforward to reconcile the effects of certain mutations on protein stability. For example, charge inversion in E323K appears to cause only a moderately destabilizing effect but as noted above, the opposite charge inversion in K423E results in a severely compromised protein. Similarly, substitution of I477, to a Ser, a small polar residue, results in a low stability protein, whereas a less detrimental effect is seen when the similarly small G367 is replaced with the large, positively charged, Arg.

All Group B variants can be rescued to at least WT stability by the addition of 3M TMAO (Table 1) and most OLF mutants in this range unfold with sharp transitions, suggestive of two-state transitions. Two exceptions are C433R and I499F, which exhibit shallower unfolding transitions, implicating possible intermediates in the unfolding pathway. In the case of the invariant cysteine at position 433 (Figure 1), the single disulfide bond (36, 37) is disrupted and could result in a change in unfolding pathway. We note, however, that the C433R variant is a well-behaved monomer in solution; no heterodimerization by oxidation of the lone cysteine 245 has been observed (not shown), suggesting that the WT OLF disulfide bond is not surface-accessible. By contrast, the observed result for I499F may be an artefact of interactions with the Sypro Orange dye. Although the T_m values measured by DSF and CD (Supplemental Table S2) are similar to one another, a more cooperative transition is observed by CD, with no obvious difference in T_m measured at either of the two spectral features (Supplemental Figure S3d). In addition, this region of OLF is not part of the identified core structural domain (40).

Finally, in terms of solubility of aggregates, most myocilin variants in this group were previously found to produce insoluble aggregates according to the TX100 assay (see Table 1), with the exception of four variants that partitioned into both the soluble and insoluble fractions: I499F and G364V as well as D380A and T377M. The latter two variants are the most stable of Group B; their behavior is consistent with a general trend of increasing TX100 solubility with T_m (see Discussion). Group B variants also exhibit little or no secretion at 37 °C, but with the exception of C433R and S502P, are secreted to some degree

at 30 °C (see Table 1). In terms of age of diagnosis, there is a wide variation between 15 and 52, with an average of 29.

Most stable variants (Group C)

Of the annotated disease-causing mutants we studied, three (A427T, G246R, and A445V) unfold within 2 °C of WT OLF (T_m = 52.7 ± 0.8 °C (36)) in the absence of TMAO, indicating they have WT like stability (p-value > 0.8). These variants were further probed for structural changes by CD and found to be comparable to those of WT OLF (Figure 3a). The ratio of aggregate to monomer isolated as part of the purification procedure is higher for these three mutants than WT, however (Figure 3b, Supporting Figure S1, see Discussion). The three SNP variants (K398R, E396D, E352Q), which were identified through genome-wide sequencing efforts and are not associated with glaucoma, exhibit stability that is similar to, or exceeds, that of WT OLF. Comparison of the CD spectra of cleaved OLF SNP variants reveals no significant differences in structure (Figure 3a). In contrast to the other WT-like disease-causing mutants, the ratio of aggregate to monomer for SNPs is at least as favorable as WT OLF (Figure 3c). Finally, Group C OLF variants exhibit WT OLF behavior in the solubility and cell secretion assays, namely high solubility in TX100 and ample secretion at 37 °C (Table 1). The main outlier in this group is G246R (see below). This group of variants also exhibits a broad range of age of diagnosis with an average of 52 years and span from 20 to 73 years.

Discussion

Trends

Taken together (Table 2), Group A comprises the least stable variants that are largely insoluble, cause the most severe cellular effects, and overall, have the earliest diagnosis of glaucoma. Those variants in Group B are in the intermediate range of glaucoma cases in terms of stability, age of diagnosis, and cellular defects. Mutant proteins in this group correspond to myocilin aggregates that are soluble or partially soluble in the TX100 assay and mutant myocilin that can be secreted to some extent from cells cultured at 30 °C. For Group C, variants exhibit WT levels of stability, cellular secretion, were soluble in TX100, and receive the latest diagnosis of glaucoma. All OLF variants we have examined to date by CD retain similar secondary structure to wild-type OLF.

With a substantial protein stability dataset now in hand, the statistical significance of specific trends can be evaluated. First, given the caveat that ‘age of diagnosis’ is the best available proxy for ill-defined parameters of ‘age of onset’ and ‘disease severity’ for glaucoma patients, the parameter is positively correlated with T_m (correlation coefficient = 0.54, statistically non-zero slope = 0.154, p-value < 0.0005, Figure 4a). Age of diagnosis is expected to vary among patients because (a) glaucoma is painless and can go unnoticed until loss of visual field occurs; asymptomatic patients under 40 years of age are rarely examined by ophthalmologists (10) and (b) age data are only available for a subset of recorded variants. In addition, the ‘age of diagnosis’ value for a patient harboring WT OLF is not defined, but the trend is supported if WT OLF (52.7 °C) were included for an age above 40 years, the threshold for adult-onset open angle glaucoma (1). Second, in terms of aggregates categorized by the TX100 assay, there is a difference between the T_m of variants with insoluble or partially insoluble aggregates and the T_m of variants with soluble aggregates (p-values = 0.0002 and 0.0009, respectively, Figure 4b). Similarly, poorly secreted myocilins at 37 °C or 30 °C exhibit lower OLF T_m values than their well-secreted counterparts (for non-secretion versus secreted at 37 °C, p = 0.0022 and for 30 °C, p = 0.01, Figure 4c,d). Overall, correlations between T_m and aggregation/non-secretion are consistent with the definition of T_m, which relates to the relative balance of unfolded protein compared to folded at a given

temperature; the higher the proportion of unfolded protein, the greater the exposure of interior hydrophobic and aggregation-prone residues.

Outliers

In spite of trends for most myocilin variants, the presence of several outliers indicates that biophysical properties other than protein stability may be involved in myocilin glaucoma as well. First, three amino acid substitutions observed in the moderately stable group, R272G, N480K, and P481L, result in a poor response to stabilization by TMAO. On average, 3M TMAO exerts an impressive and consistent +10 °C improvement in stability on WT and nearly all mutant OLFs, but these outliers lie well outside the lower boundary for the 95% confidence interval and one standard deviation below the mean (Figure 4e). Sequence alignment with myocilin from other organisms (Figure 1) reveals that these three positions are highly conserved, suggesting they are key to structural integrity of OLF. Among the six species aligned, R272 is substituted only once, in *D. rerio* (Gln), and the other two residues are invariant. It is possible that an interaction utilizing the side chain of Arg or Asn contributes significantly to overall stability, and effects of TMAO on the polypeptide main chain cannot compensate for the loss of either of these interactions. In addition, conformationally restrictive Pro residues are typically found in specialized roles in the polypeptide backbone that cannot be filled by a Leu substitution.

Second, aggregates of the moderately stable variants G364V and I499F are partially soluble in the TX100 assay whereas all but the most stable variants in this group are insoluble in the assay. Another common factor between these two variants is their low, but detectable, secretion from cells at 37 °C. In the well-studied non-ocular myocilin homolog, *S. purpratus* amassin, G364 is replaced with Asp, suggesting that in principle, a smaller side chain, such as Val, may be accommodated. In the case of the I499F variant, other hydrophobic residues Val (*D. rerio*) and Leu (*S. purpuratus*) are tolerated in this position, suggesting Phe should be tolerated as well. Genetic evidence consistent with the finding of favorable solubility and secretion behavior for I499F is incomplete penetrance; within a single family, only seven of nine individuals harboring this mutation were diagnosed with glaucoma (42). However, a molecular rationale for favorable solubilization and secretion behavior of these two moderately stable OLF variants is not apparent and remains an open area for further investigation.

Third, unlike all other moderately stable variants that exhibit some secretion from cells cultured at 30 °C, inexplicably, C433R and S502P, do not. One possibility for this phenotype is that the resulting aggregates are particularly harmful. Any unfolding intermediates (see Results, Figure 2) in C433R may stably expose part of its hydrophobic core that could inadvertently recruit other nascent polypeptides prior to aggressively forming inclusions, for example. For S502P, alteration to the inflexible Pro residue may compromise the structural integrity of this C- terminal domain (40), although smaller and larger amino acids, charged and hydrophobic, appear to be tolerated in this position (see Figure 1).

Lastly, it is curious that certain mutants exhibit WT OLF stability, CD spectral features, aggregate solubility, and cell secretion profile. At first glance, it might be tempting to dismiss disease-causing Group C variants as mislabeled. To the best of our knowledge and unlike the SNP variants, A427T and G246R have been reported just once, A445V, twice (Table 1), and individuals reported to harbor the A427T or A445V substitution received a diagnosis at 63 and 73 years of age, respectively (43), outside the threshold for ‘early-onset’ glaucoma (1) (Table 1). However, upon closer inspection, there are differences between WT OLF and G246R, A427T, A445V that suggest they may be pathogenic. First, G246R is an outlier in stabilization enhancement by TMAO (Figure 4e); other variants with Gly to Arg mutations (G252R, G367R) are less stable but do not share this feature. G246R is also an

outlier in terms of the TX100 (Figure 4b) and cell secretion assays (Figure 4c,d). In addition, although the phenomenon is not understood, all OLF variants expressed and purified to date in *E. coli* exhibit a characteristic, non-interconverting, and reproducible ratio of void volume-to-monomer peak ratio (see (36) and Supporting Figure S1), with higher relative yield of monomer for non-pathogenic compared to disease-causing variants. The SEC profiles for G246R, A427T and A445V follow the less favorable ratio similar to disease-causing variants, and not that of the SNPs (Figure 3b,c). In sum, these variants appear to harbor defects that manifests in SEC but not captured by protein stability, the details of which will need to be investigated further.

Comparison to other protein conformational disorders

The findings for OLF variants in this study fit well with trends observed in other diseases of protein misfolding in which pathogenic variants exhibit compromised thermal stability, impaired biological function, changes in kinetics of folding, and/or folding pathway. For example, more than 150 temperature-sensitive, oncogenic p53 mutants have been identified (44–46). However, some mutations localize to a loop in p53 decrease its DNA-binding, an activity critical to its function as a transcription factor, without appreciably destabilizing the overall protein (46). The specifics of the mutation in p53 correlate with breast cancer prognosis and response to treatment (47). Similarly, numerous (29), but not all, ALS-provoking SOD1 mutations alter protein stability (48). One of the most prevalent SOD1 variants found in North America, A4V, is an example of a non-destabilized variant (49). Mapped onto the SOD1 structure, pathogenic mutations in the main β-barrel typically lead to destabilized SOD1, whereas variants on the metal binding loop do not affect protein stability (49). Notably, there is limited consensus on the mechanism by which a particular SOD1 mutant becomes aggregation-prone and pathogenic (50). For example, changes in net repulsive charge on SOD1 have been shown to trigger (51) or be protective of (50, 52) pathogenic behavior. In addition, it is unclear whether aggregates are even the toxic species (53). Finally, in neonatal onset diabetes mellitus, mutations that introduce an additional cysteine residue in proinsulin (30) lead to disulfide shuffling and kinetic trapping of misfolded intermediates (54). Yet, non-cysteine missense mutations in proinsulin, located in a region not even present in mature, processed, insulin, can alter folding efficiency (55).

In sum, this study of OLF variants reveals general relationships between protein stability, age of diagnosis, and protein behavior, and identifies notable outliers, as well as certain variants with traits indistinguishable from WT. These complexities are paralleled in other protein conformational disorders and should prompt further work to assess the contribution of biophysical properties other than protein stability, such as folding pathways or kinetics, in myocilin glaucoma. In the long term, complementary functional and structural studies will also be required to fully comprehend the effects of mutations on the OLF domain of myocilin, which together may ultimately enable therapeutic intervention.

Supplementary Material

Refer to Web version on PubMed Central for supplementary material.

Acknowledgments

This work was supported by grants from the Glaucoma Research Foundation; the American Health Assistance Foundation; NIH (R01EY021205); and a Pew Scholar in the Biomedical Sciences award to R. L. L., as well as a National Science Foundation Research Experiences of Undergraduates in Chemistry at Georgia Institute of Technology (0851780) award to C. A. W. The authors gratefully acknowledge the Parker H. Petit Institute for Biosciences Core facility for access to the RT-PCR and to the Hud lab for use of their CD spectropolarimeter.

Abbreviations

ALS	amyotrophic lateral sclerosis
CD	circular dichroism
DSF	differential scanning fluorimetry
ER	endoplasmic reticulum
MBP	maltose binding protein
OLF	Olfactomedin
SEC	size exclusion chromatography
SNP	single nucleotide polymorphism
TEM	trabecular extracellular matrix
T_m	melting temperature
TMAO	trimethyl amine-N-oxide
TX100	Triton X-100

References

1. Kwon YH, Fingert JH, Kuehn MH, Alward WL. Primary open-angle glaucoma. N Engl J Med. 2009; 360:1113–1124. [PubMed: 19279343]
2. Gong G, Kosoko-Lasaki O, Haynatzki GR, Wilson MR. Genetic dissection of myocilin glaucoma. Hum Mol Genet. 2004; 13:R91–102. [PubMed: 14764620]
3. Tamm ER. Myocilin and glaucoma: facts and ideas. Prog Retin Eye Res. 2002; 21:395–428. [PubMed: 12150989]
4. Resch Z, Fautsch M. Glaucoma-associated myocilin: A better understanding but much more to learn. Exp Eye Res. 2009; 88:704–712. [PubMed: 18804106]
5. Tamm ER, Russell P, Epstein DL, Johnson DH, Piatigorsky J. Modulation of myocilin/TIGR expression in human trabecular meshwork. Invest Ophthalmol Vis Sci. 1999; 40:2577–2582. [PubMed: 10509652]
6. Jacobson N, Andrews M, Shepard AR, Nishimura D, Searby C, Fingert JH, Hageman G, Mullins R, Davidson BL, Kwon YH, Alward WL, Stone EM, Clark AF, Sheffield VC. Non-secretion of mutant proteins of the glaucoma gene myocilin in cultured trabecular meshwork cells and in aqueous humor. Hum Mol Genet. 2001; 10:117–125. [PubMed: 11152659]
7. Senatorov V, Malyukova I, Fariss R, Wawrousek EF, Swaminathan S, Sharan SK, Tomarev S. Expression of mutated mouse myocilin induces open-angle glaucoma in transgenic mice. J Neurosci. 2006; 26:11903–11914. [PubMed: 17108164]
8. Zhou Y, Grinchuk O, Tomarev SI. Transgenic mice expressing the Tyr437His mutant of human myocilin protein develop glaucoma. Invest Ophthalmol Vis Sci. 2008; 49:1932–1939. [PubMed: 18436825]
9. Wilkinson CH, van der Straaten D, Craig JE, Coote MA, McCartney PJ, Stankovich J, Stone EM, Mackey DA. Tonography demonstrates reduced facility of outflow of aqueous humor in myocilin mutation carriers. J Glaucoma. 2003; 12:237–242. [PubMed: 12782842]
10. Weinreb RN, Khaw PT. Primary open-angle glaucoma. Lancet. 2004; 363:1711–1720. [PubMed: 15158634]
11. Wang L, Zhuo Y, Liu B, Huang S, Hou F, Ge J. Pro370Leu mutant myocilin disturbs the endoplasm reticulum stress response and mitochondrial membrane potential in human trabecular meshwork cells. Mol Vis. 2007; 13:618–625. [PubMed: 17515882]
12. Carbone MA, Ayroles JF, Yamamoto A, Morozova TV, West SA, Magwire MM, Mackay TFC, Anholt RRH. Overexpression of myocilin in the Drosophila eye activates the unfolded protein response: implications for glaucoma. PLoS ONE. 2009; 4:e4216. [PubMed: 19148291]

13. Yam GHF, Gaplovska-Kysela K, Zuber C, Roth J. Aggregated myocilin induces russell bodies and causes apoptosis: implications for the pathogenesis of myocilin-caused primary open-angle glaucoma. Am J Pathol. 2007; 170:100–109. [PubMed: 17200186]
14. Zhou Z, Vollrath D. A cellular assay distinguishes normal and mutant TIGR/myocilin protein. Hum Mol Genet. 1999; 8:2221–2228. [PubMed: 10545602]
15. Liu Y, Vollrath D. Reversal of mutant myocilin non-secretion and cell killing: implications for glaucoma. Hum Mol Genet. 2004; 13:1193–1204. [PubMed: 15069026]
16. Vollrath D, Liu Y. Temperature sensitive secretion of mutant myocilins. Exp Eye Res. 2006; 82:1030–1036. [PubMed: 16297911]
17. Gobeil S, Letartre L, Raymond V. Functional analysis of the glaucoma-causing TIGR/myocilin protein: integrity of amino-terminal coiled-coil regions and olfactomedin homology domain is essential for extracellular adhesion and secretion. Exp Eye Res. 2006; 82:1017–1029. [PubMed: 16466712]
18. Yam GHF, Gaplovska-Kysela K, Zuber C, Roth J. Sodium 4-phenylbutyrate acts as a chemical chaperone on misfolded myocilin to rescue cells from endoplasmic reticulum stress and apoptosis. Invest Ophthalmol Vis Sci. 2007; 48:1683–1690. [PubMed: 17389500]
19. Jia LY, Gong B, Pang CP, Huang Y, Lam DSC, Wang N, Yam GHF. Correction of the disease phenotype of myocilin-causing glaucoma by a natural osmolyte. Invest Ophthalmol Vis Sci. 2009; 50:3743–3749. [PubMed: 19234343]
20. Gobeil S, Rodrigue M-A, Moisan S, Nguyen TD, Polansky JR, Morissette J, Raymond V. Intracellular sequestration of hetero-oligomers formed by wild-type and glaucoma-causing myocilin mutants. Invest Ophthalmol Vis Sci. 2004; 45:3560–3567. [PubMed: 15452063]
21. Powers ET, Morimoto RI, Dillin A, Kelly JW, Balch WE. Biological and chemical approaches to diseases of proteostasis deficiency. Ann Rev Biochem. 2009; 78:959–991. [PubMed: 19298183]
22. Kim BS, Savinova OV, Reedy MV, Martin J, Lun Y, Gan L, Smith RS, Tomarev SI, John SW, Johnson RL. Targeted disruption of the myocilin gene (myoc) suggests that human glaucoma-causing mutations are gain of function. Mol Cell Biol. 2001; 21:7707–7713. [PubMed: 11604506]
23. Lam DS, Leung YF, Chua JK, Baum L, Fan DS, Choy KW, Pang CP. Truncations in the TIGR gene in individuals with and without primary open-angle glaucoma. Invest Ophthalmol Vis Sci. 2000; 41:1386–1391. [PubMed: 10798654]
24. Resch ZT, Hann CR, Cook KA, Fautsch MP. Aqueous humor rapidly stimulates myocilin secretion from human trabecular meshwork cells. Exp Eye Res. 2010; 91:901–908. [PubMed: 20932969]
25. Mertts M, Garfield S, Tanemoto K, Tomarev SI. Identification of the region in the N-terminal domain responsible for the cytoplasmic localization of Myoc/Tigr and its association with microtubules. Lab Invest. 1999; 79:1237–1245. [PubMed: 10532587]
26. Stamer W, Perkumas K, Hoffman E. Coiled–coil targeting of myocilin to intracellular membranes. Experimental Eye Research. 2006
27. Hardy KM, Hoffman EA, Gonzalez P, McKay BS, Stamer WD. Extracellular trafficking of myocilin in human trabecular meshwork cells. J Biol Chem. 2005; 280:28917–28926. [PubMed: 15944158]
28. Joerger AC, Fersht AR. Structural biology of the tumor suppressor p53. Ann Rev Biochem. 2008; 77:557–582. [PubMed: 18410249]
29. Nordlund A, Oliveberg M. SOD1-associated ALS: a promising system for elucidating the origin of protein-misfolding disease. HFSP J. 2008; 2:354–364. [PubMed: 19436494]
30. Liu M, Hodish I, Haataja L, Lara-Lemus R, Rajpal G, Wright J, Arvan P. Proinsulin misfolding and diabetes: mutant INS gene-induced diabetes of youth. Trends Endocrinol Metab. 2010; 21:652–659. [PubMed: 20724178]
31. Grace ME, Newman KM, Scheinker V, Berg-Fussman A, Grabowski GA. Analysis of human acid beta-glucosidase by site-directed mutagenesis and heterologous expression. J Biol Chem. 1994; 269:2283–2291. [PubMed: 8294487]
32. Steet RA, Chung S, Wustman B, Powe A, Do H, Kornfeld SA. The iminosugar isofagomine increases the activity of N370S mutant acid beta-glucosidase in Gaucher fibroblasts by several mechanisms. Proc Natl Acad Sci USA. 2006; 103:13813–13818. [PubMed: 16945909]
33. Butters TD. Gaucher disease. Curr Opin Chem Biol. 2007; 11:412–418. [PubMed: 17644022]

34. Shimizu S, Lichter PR, Johnson AT, Zhou Z, Higashi M, Gottfredsdottir M, Othman M, Moroi SE, Rozsa FW, Schertzer RM, Clarke MS, Schwartz AL, Downs CA, Vollrath D, Richards JE. Age-dependent prevalence of mutations at the GLC1A locus in primary open-angle glaucoma. Am J Ophthalmol. 2000; 130:165–177. [PubMed: 11004290]
35. Barnes MR. Genetic variation analysis for biomedical researchers: a primer. Methods Mol Biol. 628:1–20. [PubMed: 20238073]
36. Burns JN, Orwig SD, Harris JL, Watkins JD, Vollrath D, Lieberman RL. Rescue of glaucoma-causing mutant myocilin thermal stability by chemical chaperones. ACS Chem Biol. 2010; 5:477–487. [PubMed: 20334347]
37. Nagy I, Trexler M, Patthy L. Expression and characterization of the olfactomedin domain of human myocilin. Biochem Biophys Res Commun. 2003; 302:554–561. [PubMed: 12615070]
38. Niesen FH, Berglund H, Vedadi M. The use of differential scanning fluorimetry to detect ligand interactions that promote protein stability. Nat Protoc. 2007; 2:2212–2221. [PubMed: 17853878]
39. Liu Y, Bolen DW. The peptide backbone plays a dominant role in protein stabilization by naturally occurring osmolytes. Biochemistry. 1995; 34:12884–12891. [PubMed: 7548045]
40. Orwig SD, Lieberman RL. Biophysical characterization of the olfactomedin domain of myocilin, an extracellular matrix protein implicated in inherited forms of glaucoma. PLoS ONE. 2011; 6:e16347. [PubMed: 21283635]
41. Alward WL, Fingert JH, Coote MA, Johnson AT, Lerner SF, Junqua D, Durcan FJ, McCartney PJ, Mackey DA, Sheffield VC, Stone EM. Clinical features associated with mutations in the chromosome 1 open-angle glaucoma gene (GLC1A). N Engl J Med. 1998; 338:1022–1027. [PubMed: 9535666]
42. Adam MF, Belmouden A, Binisti P, Brezin AP, Valtot F, Bechetoille A, Dascotte JC, Copin B, Gomez L, Chaventre A, Bach JF, Garchon HJ. Recurrent mutations in a single exon encoding the evolutionarily conserved olfactomedin-homology domain of TIGR in familial open-angle glaucoma. Hum Mol Genet. 1997; 6:2091–2097. [PubMed: 9328473]
43. Faucher M, Anctil JL, Rodrigue MA, Duchesne A, Bergeron D, Blondeau P, Cote G, Dubois S, Bergeron J, Arseneault R, Morissette J, Raymond V. Founder TIGR/myocilin mutations for glaucoma in the Quebec population. Hum Mol Genet. 2002; 11:2077–2090. [PubMed: 12189160]
44. Joerger AC, Fersht AR. Structure-function-rescue: the diverse nature of common p53 cancer mutants. Oncogene. 2007; 26:2226–2242. [PubMed: 17401432]
45. Bullock A, Henckel J, DeDecker B, Johnson C, Nikolova P, Proctor M, Lane D, Fersht A. Thermodynamic stability of wild-type and mutant p53 core domain. Proc Natl Acad Sci USA. 1997; 94:14338. [PubMed: 9405613]
46. Bullock AN, Henckel J, Fersht AR. Quantitative analysis of residual folding and DNA binding in mutant p53 core domain: definition of mutant states for rescue in cancer therapy. Oncogene. 2000; 19:1245–1256. [PubMed: 10713666]
47. Olivier M, Langerod A, Carrieri P, Bergh J, Klaar S, Eyfjord J, Theillet C, Rodriguez C, Lidereau R, Bieche I, Varley J, Bignon Y, Uhrhammer N, Winqvist R, Jukkola-Vuorinen A, Niederacher D, Kato S, Ishioka C, Hainaut P, Borresen-Dale AL. The clinical value of somatic TP53 gene mutations in 1,794 patients with breast cancer. Clin Cancer Res. 2006; 12:1157–1167. [PubMed: 16489069]
48. Shaw BF, Valentine JS. How do ALS-associated mutations in superoxide dismutase 1 promote aggregation of the protein? Trends Biochem Sci. 2007; 32:78–85. [PubMed: 17208444]
49. Seetharaman SV, Prudencio M, Karch C, Holloway SP, Borchelt DR, Hart PJ. Immature copper-zinc superoxide dismutase and familial amyotrophic lateral sclerosis. Exp Biol Med. 2009; 234:1140–1154.
50. Prudencio M, Hart PJ, Borchelt DR, Andersen PM. Variation in aggregation propensities among ALS-associated variants of SOD1: correlation to human disease. Hum Mol Genet. 2009; 18:3217–3226. [PubMed: 19483195]
51. Bystrom R, Andersen PM, Grobner G, Oliveberg M. SOD1 mutations targeting surface hydrogen bonds promote amyotrophic lateral sclerosis without reducing apo-state stability. J Biol Chem. 2010; 285:19544–19552. [PubMed: 20189984]

52. Wang Q, Johnson JL, Agar NY, Agar JN. Protein aggregation and protein instability govern familial amyotrophic lateral sclerosis patient survival. PLoS Biol. 2008; 6:e170. [PubMed: 18666828]
53. Ross CA, Poirier MA. Opinion: What is the role of protein aggregation in neurodegeneration? Nat Rev Mol Cell Biol. 2005; 6:891–898. [PubMed: 16167052]
54. Weiss MA. Proinsulin and the genetics of diabetes mellitus. J Biol Chem. 2009; 284:19159–19163. [PubMed: 19395706]
55. Liu M, Hua QX, Hu SQ, Jia W, Yang Y, Saith SE, Whittaker J, Arvan P, Weiss MA. Deciphering the hidden informational content of protein sequences: foldability of proinsulin hinges on a flexible arm that is dispensable in the mature hormone. J Biol Chem. 2010; 285:30989–31001. [PubMed: 20663888]
56. Rozsa FW, Shimizu S, Lichter PR, Johnson AT, Othman MI, Scott K, Downs CA, Nguyen TD, Polansky J, Richards JE. GLC1A mutations point to regions of potential functional importance on the TIGR/MYOC protein. Mol Vis. 1998; 4:20. [PubMed: 9772276]
57. Fingert JH, Heon E, Liebmann JM, Yamamoto T, Craig JE, Rait J, Kawase K, Hoh ST, Buys YM, Dickinson J, Hockey RR, Williams-Lyn D, Trope G, Kitazawa Y, Ritch R, Mackey DA, Alward WL, Sheffield VC, Stone EM. Analysis of myocilin mutations in 1703 glaucoma patients from five different populations. Hum Mol Genet. 1999; 8:899–905. [PubMed: 10196380]
58. Richards JE, Ritch R, Lichter PR, Rozsa FW, Stringham HM, Caronia RM, Johnson D, Abundo GP, Willcockson J, Downs CA, Thompson DA, Musarella MA, Gupta N, Othman MI, Torrez DM, Herman SB, Wong DJ, Higashi M, Boehnke M. Novel trabecular meshwork inducible glucocorticoid response mutation in an eight-generation juvenile-onset primary open-angle glaucoma pedigree. Ophthalmology. 1998; 105:1698–1707. [PubMed: 9754180]
59. Morissette J, Clepet C, Moisan S, Dubois S, Winstall E, Vermeeren D, Nguyen TD, Polansky JR, Cote G, Anctil JL, Amyot M, Plante M, Falardeau P, Raymond V. Homozygotes carrying an autosomal dominant TIGR mutation do not manifest glaucoma. Nat Genet. 1998; 19:319–321. [PubMed: 9697688]
60. Bruttini M, Longo I, Frezzotti P, Ciappetta R, Randazzo A, Orzalesi N, Fumagalli E, Caporossi A, Frezzotti R, Renieri A. Mutations in the myocilin gene in families with primary open-angle glaucoma and juvenile open-angle glaucoma. Arch Ophthalmol. 2003; 121:1034–1038. [PubMed: 12860809]
61. Stone EM, Fingert JH, Alward WL, Nguyen TD, Polansky JR, Sunden SL, Nishimura D, Clark AF, Nystuen A, Nichols BE, Mackey DA, Ritch R, Kalenak JW, Craven ER, Sheffield VC. Identification of a gene that causes primary open angle glaucoma. Science. 1997; 275:668–670. [PubMed: 9005853]
62. Vasconcellos JP, Melo MB, Costa VP, Tsukumo DM, Basseres DS, Bordin S, Saad ST, Costa FF. Novel mutation in the MYOC gene in primary open glaucoma patients. J Med Genet. 2000; 37:301–303. [PubMed: 10819638]
63. Stoilova D, Child A, Brice G, Desai T, Barsoum-Homsy M, Ozdemir N, Chevrette L, Adam MF, Garchon HJ, Pitts Crick R, Sarfarazi M. Novel TIGR/MYOC mutations in families with juvenile onset primary open angle glaucoma. J Med Genet. 1998; 35:989–992. [PubMed: 9863594]
64. Brezin AP, Adam MF, Belmouden A, Lureau MA, Chaventre A, Copin B, Gomez L, De Dinechin SD, Berkani M, Valtot F, Rouland JF, Dascotte JC, Bach JF, Garchon HJ. Founder effect in GLC1A-linked familial open-angle glaucoma in Northern France. Am J Med Genet. 1998; 76:438–445. [PubMed: 9556305]
65. Kanagavalli J, Pandaranayaka PJE, Krishnadas SR, Krishnaswamy S, Sundaresan P. In vitro and in vivo study on the secretion of the Gly367Arg mutant myocilin protein. Mol Vis. 2007; 13:1161–1168. [PubMed: 17679945]
66. Hulsman CA, De Jong PT, Lettink M, Van Duijn CM, Hofman A, Bergen AA. Myocilin mutations in a population-based sample of cases with open-angle glaucoma: the Rotterdam Study. Graefes Arch Clin Exp Ophthalmol. 2002; 240:468–474. [PubMed: 12107514]
67. Mackey DA, Healey DL, Fingert JH, Coote MA, Wong TL, Wilkinson CH, McCartney PJ, Rait JL, de Graaf AP, Stone EM, Craig JE. Glaucoma phenotype in pedigrees with the myocilin Thr377Met mutation. Arch Ophthalmol. 2003; 121:1172–1180. [PubMed: 12912696]

68. Alward WL, Kwon YH, Khanna CL, Johnson AT, Hayreh SS, Zimmerman MB, Narkiewicz J, Andorf JL, Moore PA, Fingert JH, Sheffield VC, Stone EM. Variations in the myocilin gene in patients with open-angle glaucoma. Arch Ophthalmol. 2002; 120:1189–1197. [PubMed: 12215093]

69. Melki R, Belmouden A, Brezin A, Garchon HJ. Myocilin analysis by DHPLC in French POAG patients: increased prevalence of Q368X mutation. Hum Mutat. 2003; 22:179. [PubMed: 12872267]

70. Pei J, Kim BH, Tang M, Grishin NV. PROMALS web server for accurate multiple protein sequence alignments. Nuc Acids Res. 2007; 35:W649–652.

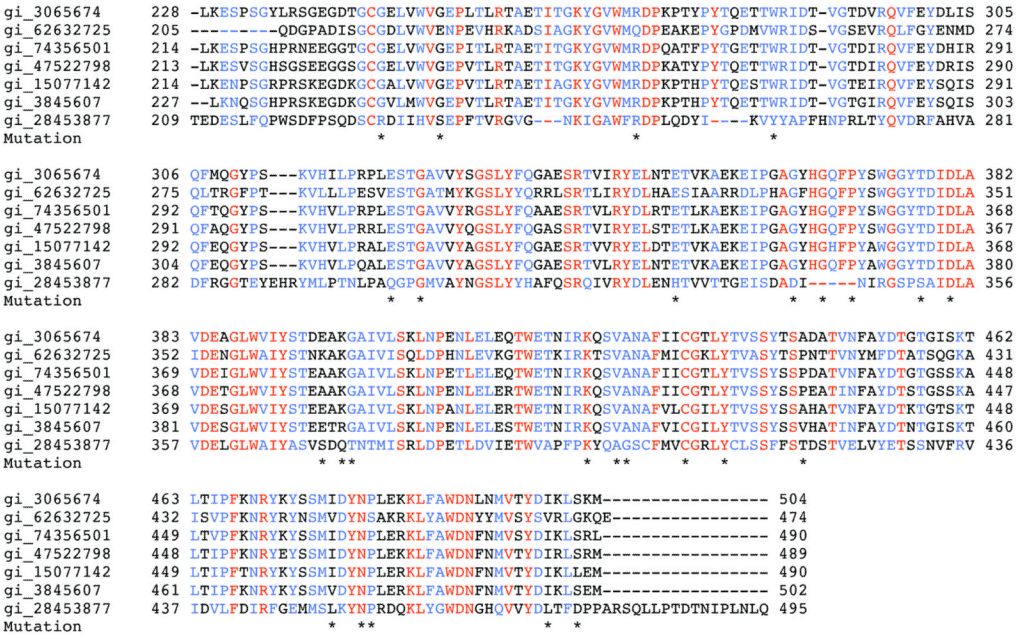

Figure 1.

Multiple sequence alignment of the myocilin OLF domain and non-ocular amassin OLF domain. Alignment includes myocilin OLF domains from *H. sapiens* (gi accession number 3065674), *D. rerio* (gi accession number 62632725), *B. taurus* (gi accession number 74356501), *S. scrofa* (gi accession number 47522798), *M. musculus* (gi accession number 15077142), *R. norvegicus* (gi accession number 3845607), and the amassin OLF domain from *S. purpuratus* (gi accession number 28453877). Blue: similar residues; Red: identical residues; asterisk: site of mutation in this study. The alignment was generated using PROMALS3D (70).

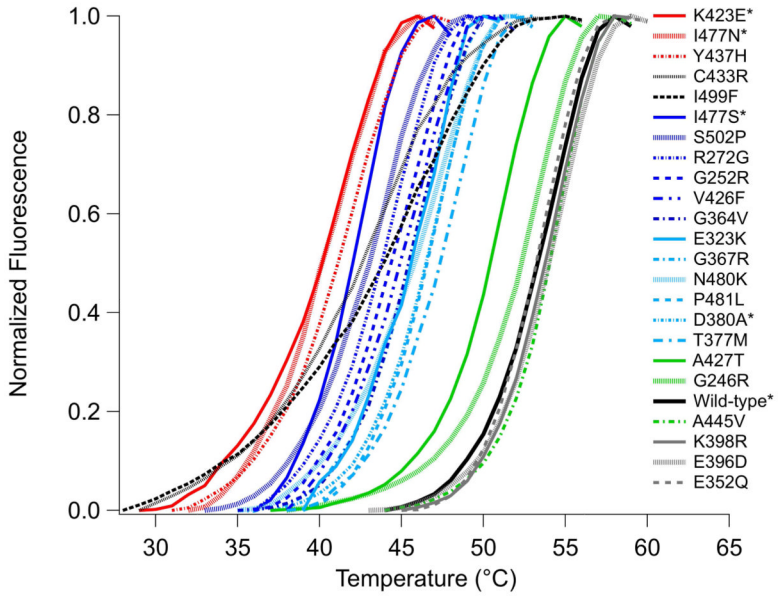

Figure 2.

Melting thermograms for myocilin OLF variants. Solid black: Wild-type OLF; Red: Group A; Blue, dashed Black: Group B; Green, Grey: Group C. Note two dashed black curves corresponding to C433R and I499F deviate from apparent two-state transition. Asterisk indicates curves published in (36). No thermograms were obtained for W286R or P370L.

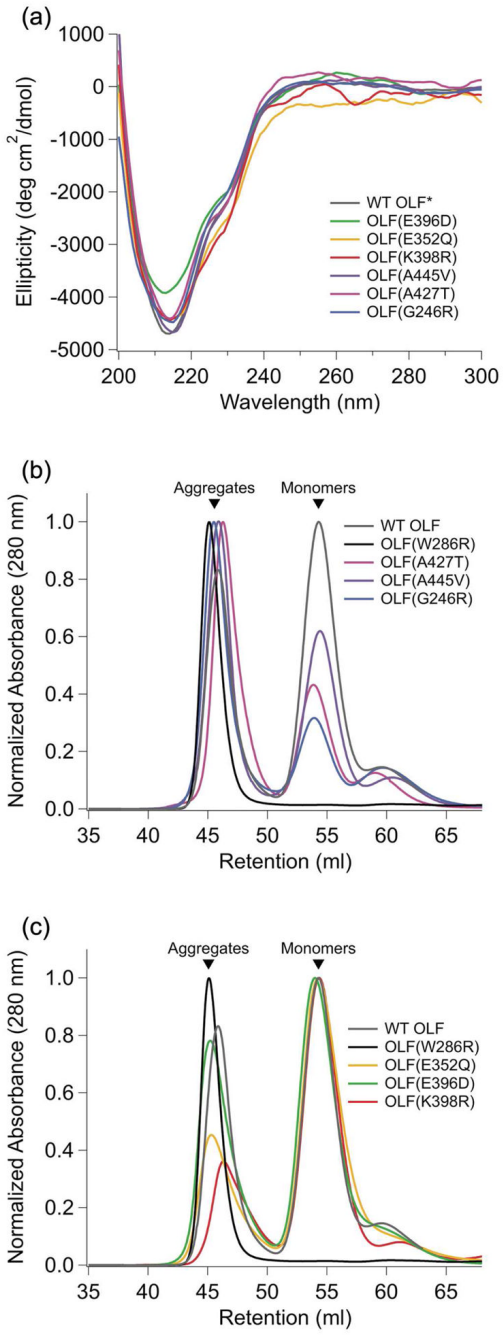

Figure 3.

Features of most stable OLF variants. (a) Circular dichroism spectra for Group C variants. Asterisk denotes spectrum for WT OLF reported in (40). (b) Comparison of relative aggregate and monomer isolated for disease-causing variants in Group C compared with W286R and WT OLF by size exclusion chromatography. (c) Comparison of relative aggregate and monomer isolated for SNP variants with WT OLF by size exclusion chromatography. Each trace has been normalized.

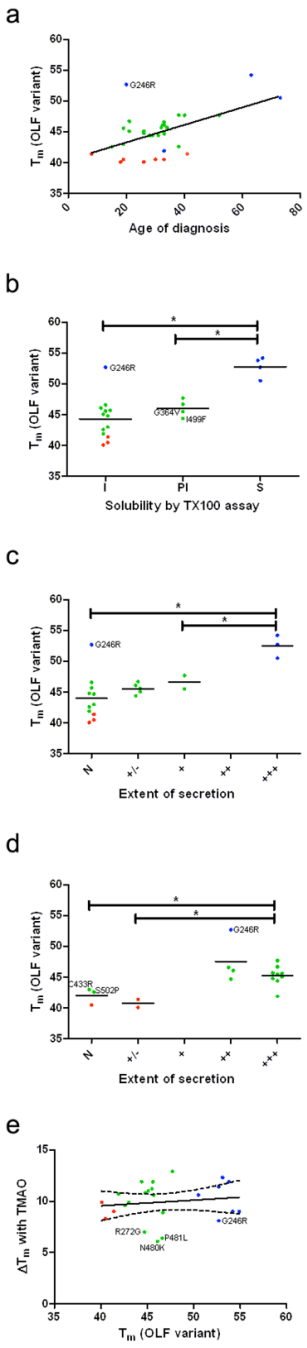

Figure 4.

Statistical analyses conducted in this study. (a) Correlation between T_m of OLF variant and age of glaucoma diagnosis, (b) Significance of T_m differences and aggregate solubility using TX100 assay, and (c, d) Significance of T_m differences and extent of secretion from cells cultured at 37 °C and 30 °C, respectively. For (b)–(d), see symbol definition in Table 1. (e) ΔT_m for each OLF variant with the addition of 3M TMAO plotted as a function of T_m without TMAO. Dashed lines indicate 95% confidence intervals and slope does not statistically deviate from zero ($p > 0.5$). Red, green, and blue colors indicate variants found in groups as defined in Table 1, outliers discussed in text are labeled. * indicates statistical difference with p-value < 0.05 as described in text.

Biochemistry. Author manuscript; available in PMC 2012 July 5.

Table 1

Compilation of data on myocilin glaucoma variants from this and previous studies. Variants are listed in order of melting temperature (T_m).

Group	Mutation			T_m		ΔT_m	Solubility Assay[b]	Secretion Assay[c]		Age(s) of Diagnosis	References[d]
				Protein only	+3M TMAO			37°C	30 °C		
	P	370	L	NA	NA	NA	I	N	+/−	12, 12, 10.5	(34), (56), (42)
	W	286	R	NA	NA	NA	NA	N	N	NA (pop.)	(57)
A	I	477	N	40.1±0.8	50.1±0.8	9.9	I	N	+/−	26, 18, 18, Pop.	(34), (56), (58), (57)
	K	423	E	40.5±0.1	48.8±0.7	8.3	I	N	N	19, 33, 30	(59), (60), (43)
	Y	437	H	41.4±0.1	50.4±1.1	9.0	I	N	+/−	NA (pop.), NA (pop.), 8–41	(57), (61), (41)
B	I	477	S	41.9±0.5	52.7±0.8	10.7	I	N	+++	33	(42)
	C	433	R	42.6±0.4	52.2±0.6	9.6	I	N	N	15, 38	(62)
	S	502	P	43.0±0.1	52.9±0.2	9.9	I	N	N	19	(63)
	I	499	F	44.4±0.3	56.3±0.3	11.9	PI	+/−	+++	28, 29, 31	(34), (64), (42)
	R	272	G	44.7±0.2	51.7±0.6	7.0	NA	N	++	33	(34)
	G	252	R	44.8±0.7	55.6±0.8	10.8	I	N	+++	26, 26	(34), (56)
	V	426	F	45.1±0.4	56.1±0.8	11.0	I	+/−	+++	21, 26	(34), (56)
	G	364	V	45.5±0.2	56.7±0.2	11.2	PI	+	+++	NA (pop., fam.)	(57), (61)
	E	323	K	45.6±0.4	57.5±0.5	11.9	I	+/−	+++	19, 19	(34), (56)
	G	367	R	45.7±0.1	56.3±0.3	10.6	I	N	+++	32, 34	(65), (43)
	N	480	K	46.1±0.3	52.2±0.8	6.1	I	+/−	++	30/35/32, 30/34/40	(42), (66)
	P	481	L	46.6±0.1	53.0±0.8	6.4	I	N	++	33, NA (pop.)	(43), (57)
	D	380	A	46.7±0.5	55.6±0.9	8.9	PI	+/−	+++	21	(63)
	T	377	M	47.7±0.2	60.6±0.7	12.9	PI	+	+++	38, 52, 40, NA (pop.)	(34), (65), (67), (57)
	A	427	T	50.5±0.2	61.1±0.4	10.6	S	+++	NA	73	(43)
	G	246	R	52.7±0.5	60.8±0. 7	8.1	I	N	++	20	(42)
	Wild-type			52.7±0.8	64.1±0.7	11.4	S	+++	NA	--	--
C	K	398	R	53.8±0.2	62.2±0.2	11.9	S	NA	NA	rs56314834[a]	(57), (68), (34), (43), (69), (66)
	E	396	D	53.1±0.1	61.9±0.1	12.3	NA	NA	NA	rs61730975[a]	NA
	A	445	V	54.2±0.2	63.2±0.6	9.0	S	+++	NA	63, NA (pop.)	(43), (57)
	E	352	Q	54.9±0.5	63.1±0.4	9.0	NA	NA	NA	rs61745146[a]	NA

NA= not available; -- = not applicable; TMAO = trimethylamine N-oxide; I = insoluble; PI = partially insoluble; S = soluble; N = No secretion; +/− = little secretion; +, ++, +++ = increasing amounts of secretion as defined in (17); for age of diagnosis, commas separate ages reported in order listed references, with/to indicate multiple ages reported, pop. indicates population study with no age of diagnosis provided, and fam. indicates familial study, no age of diagnosis provided.

*Accession numbers for Database of Single Nucleotide polymorphisms (dbSNP, Build ID 131). Bethesda (MD): National Center for Biotechnology Information, National Library of Medicine. Available from: http://www.ncbi.nlm.nih.gov/SNP.

†Data from (14) and/or (34).

‡Data from (16) and/or (17).

#References refer to, and are listed in, the order of age of diagnosis.

Table 2

Overall trends of protein stability with aggregate solubility assay, secretion assay, average age of diagnosis

	T_m	Solubility of aggregates in TX100	Cell Secretion	Average age of Diagnosis
Group A	Lowest	Insoluble	Limited at 30 °C	19
Group B	Moderate	Insoluble or partially insoluble	Some at 30 °C	29, highly variable
Group C	Wild-type	Largely soluble	Secretion at both 37 °C and 30 °C	52